PROCEEDINGS OF SCIENCE

Cross section measurement of ^{209}Bi(n,γ)^{210}Bi^{g} and s−process abundance predictions in low-mass AGB stars

Bisterzo, Sara*
Dipartimento di Fisica Generale, Università di Torino, via P. Giuria 1, 10125 (To), Italy
Forschungszentrum Karlsruhe, Institut für Kernphysik, D-76021Karlsruhe, Germany
E-mail: bisterzo@ph.unito.it

Käppeler, Franz
Forschungszentrum Karlsruhe, Institut für Kernphysik, D-76021Karlsruhe, Germany
E-mail: franz.kaeppeler@ik.fzk.de

Gallino, Roberto
Dipartimento di Fisica Generale, Università di Torino, via P. Giuria 1, 10125 (To), Italy
E-mail: gallino@ph.unito.it

Heil, Michael
Forschungszentrum Karlsruhe, Institut für Kernphysik, D-76021Karlsruhe, Germany
E-mail: michael.heil@ik.fzk.de

Domingo-Pardo, Cesar
Forschungszentrum Karlsruhe, Institut für Kernphysik, D-76021Karlsruhe, Germany
E-mail: cesar.domingo@ik.fzk.de

The main-s process component, which produces the s abundances from Sr to Pb/Bi, occurs in low-mass thermally pulsing AGB stars. In this scenario, the ^{13}C$(\alpha,n)^{16}$O reaction, which burns radiatively at $T\sim 0.9\cdot 10^{8}$ K during the interpulse period, constitutes the major neutron source. A second weaker neutron source, the ^{22}Ne$(\alpha,n)^{25}$Mg, is partially activated during the convective thermal pulses, when the maximum temperature at the bottom of the He-burning shell reaches a value of $T\sim 3\cdot 10^{8}$ K. Using improved stellar (n,γ) cross sections and stellar AGB models with a full reaction network we report on an updated reproduction of the solar main-s component. We also present the status of a measurement of the ^{209}Bi(n,γ)^{210}Bi^{g} cross section, which aims at reducing the uncertainties to about 2%, and improving the accuracy of the abundances prediction at the termination point of the s−path.

International Symposium on Nuclear Astrophysics — Nuclei in the Cosmos — IX
June 25-30 2006
CERN, Geneva, Switzerland

* Speaker.

PoS(NIC-IX)077

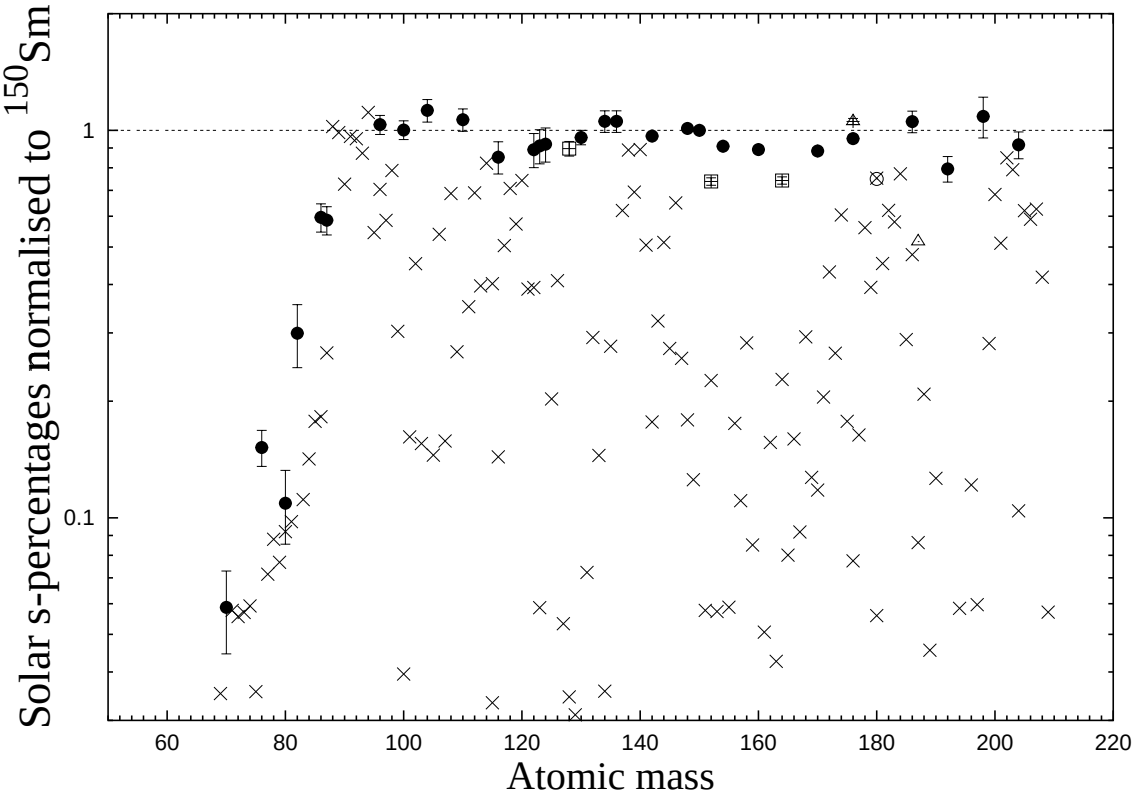

Figure 1: The s−process abundance distribution from stellar models, which best reproduce the solar system main-s component with updated cross sections. We used a standard ^{13}C-pocket, a metallicity of [Fe/H] = −0.3 and an average between M = 1.5 $M_{\odot}$ and M = 3 $M_{\odot}$. The full circles are the s-only nuclei. We adopted empty squares symbols for ^{128}Xe, ^{152}Gd and ^{164}Er, triangles for ^{176}Lu and ^{187}Os, and open circle symbol for ^{180}Ta (see text for explanations).

1. s−process in low mass AGB stars

Asymptotic Giant Branch (AGB) stars with $M \leq 4M_{\odot}$ are the site of the main s process. We investigate the s−process contribution to the various isotopes of this region using the FRANEC code with a full network, from hydrogen to lead and bismuth, which includes (n, γ), (n, α), (n, p) cross sections and β-decay rates, all updated by the latest experimental results. In a previous study it was shown that the main component can be reproduced by a standard ^{13}C-pocket, a metallicity of [Fe/H] = −0.3, and an average between M = 1.5 $M_{\odot}$ and M = 3 $M_{\odot}$ ([2, 9]). For the neutron capture network, the cross sections by [4] were used, with updated experimental data and theoretical estimates (see [9] for further details). The solar isotope abundances adopted for reference were the meteoritic values by [1].

In this work, the recommended (n, γ) rates [3] were adopted, complemented by recent measurements on ^{151}Sm [18], Eu [5], ^{60}Ni [6], Kr [8], Si [11], Cl [10], Pt [16], ^{88}Sr [15], ^{139}La [31] and [20], ^{62}Ni [19], Pm [25], Xe [24], Cd [32], Hf [34], Lu [33], and using the ^{176}Lu/^{176}Hf branching from [30] as well as unpublished results for the cross sections of ^{19}F, ^{21}Ne, ^{23}Na, ^{27}Al, ^{46}Ca, ^{155}Eu, ^{160}Gd, ^{59}Co, ^{63,65}Cu, ^{79,81}Br, ^{87}Rb (M. Heil, priv. comm.). The rates of (n, α) and (n, p) are taken from [23] for the heavy isotopes, and from various authors for the light isotopes [9]. For β-decay

Table 1: Main-s process prediction from AGB stellar model (in % of the solar abundances).

El	this work	from [2]	El	this work	from [2]	El	this work	from [2]
Cu	1.3	1.0	Cd	63.4	52.0	Ho	8.0	7.8
Zn	0.8	0.9	In	38.5	35.0	Er	18.3	17.0
Ga	4.4	4.5	Sn	64.3	65.0	Tm	12.7	13.0
Ge	5.4	6.0	Sb	24.8	25.0	Yb	39.5	33.0
As	3.6	4.6	Te	17.9	17.0	Lu	20.0	20.0
Se	8.6	8.9	I	5.3	5.3	Hf	55.1	56.0
Br	8.7	9.0	Xe	16.7	17.0	Ta	45.3	41.0
Kr	16.2	19.0	Cs	14.5	15.0	W	62.0	56.0
Rb	20.2	22.0	Ba	83.4	81.0	Re	16.2	8.9
Sr	94.3	85.0	La	69.2	62.0	Os	9.8	9.4
Y	98.7	92.0	Ce	80.8	77.0	Ir	1.5	1.4
Zr	85.8	83.0	Pr	50.6	49.0	Pt	6.4	5.1
Nb	87.2	85.0	Nd	56.9	56.0	Au	6.0	5.8
Mo	51.0	50.0	Sm	31.0	29.0	Hg	64.2	61.0
Ru	33.9	32.0	Eu	5.7	5.8	Tl	67.1	76.0
Rh	15.5	14.0	Gd	11.1	15.0	Pb	51.5	46.0
Pd	34.3	46.0	Tb	8.5	7.2	Bi	5.7	4.9
Ag	14.8	20.0	Dy	14.5	15.0			

we used [26], with exception of ^{79}Se [13] and ^{176}Lu [14]. For the ^{176}Lu and ^{176}Hf branchings an improved treatment has been applied [30].

In Figure 1 we show the solar s−process abundance distribution normalised to the s-only nucleus ^{150}Sm. The solar abundances are from [17], with the exception of Zr, which was adopted from [12]. The full circles are the s-only nuclei. We adopted different symbols for ^{128}Xe, ^{152}Gd, and ^{164}Er, which have a not negligible p contribution (10 % for Xe), for ^{176}Lu, a long-lived isotope (3.8 x 10^{10} y) which decays into ^{176}Hf, for ^{187}Os, which is affected by the long-lived decay of ^{187}Re (5 x 10^{10} y), and for ^{180}Ta, which receives also contributions from the p-process and from ν-interactions in massive stars. The error bars account for the uncertainties of the solar abundances alone. The major differences between this and previous work [2] refer to the Xe isotopes, for which we adopted the solar value from [24], and for the ^{176}Lu/^{176}Hf branching (see [30] for a discussion). Some discrepancies for ^{116}Sn, ^{154}Gd, ^{160}Dy, ^{170}Yb, and ^{192}Pt suggest that better cross sections including their stellar enhancement factor (SEF) [23], are important for isotopes with A $\gtrsim$ 150 in order to obtain more detailed branching analyses. The derived s−process contributions to the solar abundances are reported in Table 1. The updated s−process calculations will be compared with a GCE model [27, 28, 29], which considers the chemical evolution of stars in the mass range between 1 and 8 solar masses in three galactic zones (halo, thick, and thin disk) over the galactic history. Subtracting the s−process contributions from the solar abundances yields an improved determination of the r-process isotopic and elemental abundance distribution in the mass range A

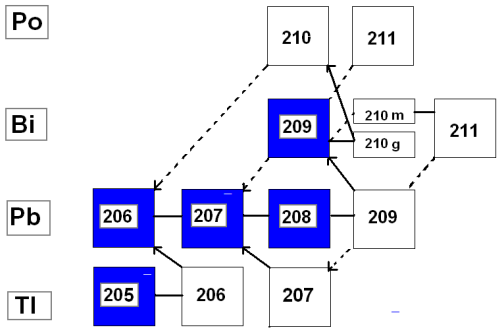

Figure 2: The s−process path in the region of Pb/Bi. The stable isotopes are indicated in blue.

$>$ 90, which has a profound impact on r-process predictions and in particular on the spectroscopic analyses of very metal-poor stars with strongly enhanced r-process signatures.

2. Cross section measurement of ^{209}Bi(n, γ)^{210}Bi^{g}

^{209}Bi is the last stable isotope in the s−path, before the region of the α-unstable isotopes. Neutron capture on ^{209}Bi feeds the short-lived ground state of ^{210}Bi ($t_{1/2}$ = 5.013 d), which decays to ^{210}Po ($t_{1/2}$ = 138.38 d), as well as the isomer ^{210}Bi^{m}, which is α-unstable with a long half-life (3 x 10^{6} yr). The total ^{209}Bi(n, γ) cross section was recently measured at the CERN n_TOF facility [7]. The partial cross section to the ground state is known with an uncertainty of about 6 % [21]. A reduction of this uncertainty is necessary to understand the recycling via α-decay of ^{210,211}Po and the corresponding accumulation of s−process material (Figure 2). Moreover, a more accurate isotopic abundance in this region will consolidate the reliability of the Th and U chronometers.

The measurement of this cross section is carried out by the activation method, which is well suited to determine very small cross sections at magic neutron number. The neutron activation method consists of two steps: neutron irradiation of the sample and the counting of the induced activity. In our case the measurement presents some differences with respect to typical activations: because the γ line produced from the β-decay of ^{210}Bi is too weak, the induced activities can not be detected via γ-spectroscopy with Ge detectors. Therefore, we followed the α-decay of ^{210}Po with a low-background α-detector. Bi samples 10 mm in diameter and 3 micrometer in thickness were prepared by evaporation of a high-purity Bi metal. During the irradiations, the Bi samples were sandwiched between gold foils for defining the flux via the gold cross section standard. The measurement was carried out in a quasi-Maxwellian neutron spectrum with kT = 25 keV by employing the ^{7}Li(p, n)^{7}Be reaction at E$_p$ = 1921 keV. This proton energy is just above the reaction threshold, to obtain a kinematically collimated neutron beam in a forward cone with an opening angle of 120°. In this way, disturbing scattering of the primary neutron beam in the vicinity of the sample is avoided. The irradiations were carried out using the 3.7 MV Van de Graaff accelerator at Forschungszentrum Karlsruhe. A schematic setup is given in Figure 3. A ^{6}Li glass detector was used to monitor the neutron flux during the experiment. This permits us to estimate

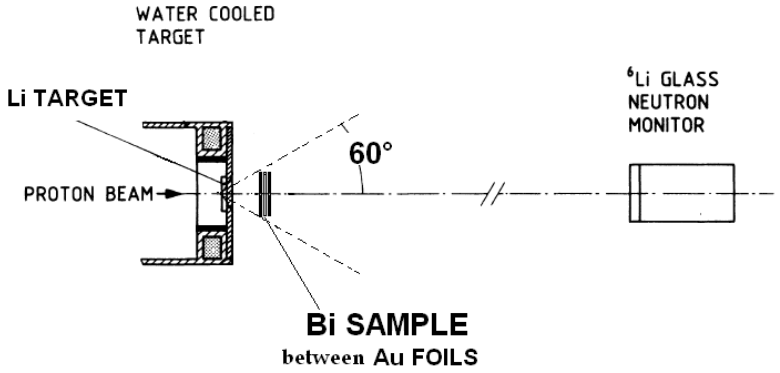

Figure 3: Schematic setup of the activation measurement at the Van de Graaff accelerator.

the correction factor f_b, which takes account of the α decay occurring already during the activation. Figure 4 shows the α-spectrum from the first irradiation after a counting period of three days.

Further activations are required to confirm the result. It is also planned to perform this measurement via Accelerator Mass Spectrometry (AMS) for a consistent assessment of the uncertainty. As shown in Table 1 the main s component provides 58% of the solar Pb and 7% of the solar Bi, according to the adopted stellar model. Additional contributions from the strong s component have to be added. The total s−process contribution to solar Pb amounts to 86.5% and to 19% of the solar Bi. The strong component is produced by AGB stars of low metallicity, and has been obtained with a Galatic Chemical Evolution (GCE) model [28]. In good approximation, this contribution correspond to the production of a stellar model of $M^{ini} = 3\ M_{\odot}$ and [Fe/H] = −1.3 [21].

References

[1] Anders, E. and Grevesse, N., 1989, Geochim. et Cosmochim. Acta 53, 197
[2] Arlandini, C. et al. 1999, ApJ, 525, 886
[3] Bao, Z. K. et al. 2000, ADNDT 76, 70
[4] Beer, H., Voss, F. and Winters, R. R. 1992, ApJS 80, 403
[5] Best, J. et al. 2001, Phys. Rev. C 64, 0115801
[6] Corvi, F. et al. 2002, Nucl. Phys. A 697, 581
[7] Domingo-Pardo, C., et al 2006, Phys. Rev. C (in press)
[8] Fazio, C. et al. 2003, GeCAS 67, 91
[9] Gallino, R. et al. 1998, ApJ 497, 388
[10] Guber, K. H. et al. 2002, Phys. Rev. C 65, 058801
[11] Guber, K. H. et al. 2003, Phys. Rev. C 67, 062802
[12] Kashiv, Y. et al. 2006, Lunar and Planetary Science XXXVII 2464
[13] Klay, N. and Käppeler, F. 1988, Phys. Rev. C 38, 295
[14] Klay, N. et al. 1991, Phys. Rev. C 44, 2839
[15] Koehler, P. E. et al. 2000, Phys. Rev. C 62, 055803
[16] Koehler, P. E. et al. 2002, JNSTS 2, 256
[17] Lodders, K. 2003, ApJ 591, 1220
[18] Marrone, S. et al. 2006, Phys. Rev. C 73, 034604

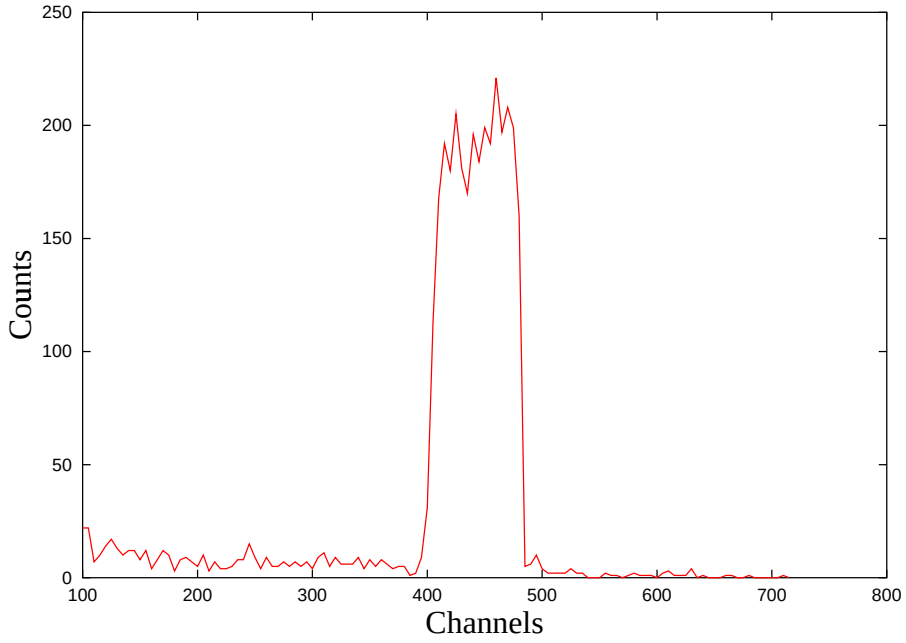

Figure 4: The α-spectrum of the activated Bi sample.

[19] Nassar, H. et al. 2005, Phys. Rev. Lett. 94, 092504
[20] O'Brien, S. et al. 2003, Phys. Rev. C 68, 035801
[21] Ratzel, U. et al. 2004, Phys. Rev. C 70, 065803
[22] Ratynski, W. and Kaeppeler, F. 1988, Phys. Rev. C 37, 2
[23] Rauscher, T. and Thielemann, F. K., 2000, Atomic Data and Nuclear Data Tables 75, 1
[24] Reifarth, R. et al. 2002, Phys. Rev. C 66, 064603
[25] Reifarth, R. et al. 2003, ApJ 582, 1251
[26] Takahashi, K. and Yokoi, K. 1987, ADNDT 36, 375
[27] Travaglio, C. et al. 1999, ApJ 521, 691
[28] Travaglio, C. et al. 2001, ApJ 549, 346
[29] Travaglio, C. et al. 2004, ApJ 601, 864
[30] Käppeler, F. et al. 2006, Mem. Soc. Astron. It 77, 916
[31] Winckler, N. et al. ApJ (in press)
[32] Wisshak, K. et al. 2002, Phys. Rev. C 66, 025801
[33] Wisshak, K. et al. 2006, Phys. Rev. C 73, 015807
[34] Wisshak, K. et al. 2006, Phys. Rev. C 73, 45807